



0062940

CR  
168920  
c.1

OLD DOMINION UNIVERSITY RESEARCH FOUNDATION

DEPARTMENT OF MECHANICAL ENGINEERING AND MECHANICS  
SCHOOL OF ENGINEERING  
OLD DOMINION UNIVERSITY  
NORFOLK, VIRGINIA

CONTROL OF LARGE SPACE STRUCTURES AND  
ASSOCIATED PRECISION-POINTED PAYLOADS

By

S.M. Joshi

G.L. Goglia, Principal Investigator

Annual Progress Report  
For the period February 15, 1981 to February 14, 1982

Prepared for the  
National Aeronautics and Space Administration  
Langley Research Center  
Hampton, Virginia

Under  
Research Grant NAG-1-102  
Harold A. Hamer, Technical Monitor  
Flight Dynamics and Control Division

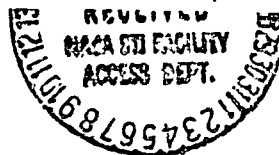
LOAN COPY: RETURN TO  
AFWL TECHNICAL LIBRARY  
KIRTLAND AFB, N.M. 87117

(NASA-CR-168920) CONTROL OF LARGE SPACE  
STRUCTURES AND ASSOCIATED PRECISION-POINTED  
PAYLOADS Annual Progress Report, 15 Feb.  
1981 - 14 Feb. 1982 (Old Dominion Univ.,  
Norfolk, Va.) 25 p HC A02/ME A01

N82-24200

Unclass  
09939

CSCL 22B G3/18



May 1982

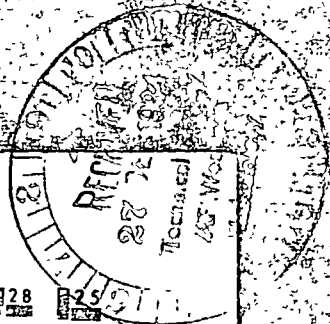


NASA  
CP  
168920

# 1 OF 1

TECH LIBRARY KAFB, NIA  
0062940

# N82-24280 UNCLAS



	1.0		2.8		2.5
	1.1		3.2		2.2
	1.1		3.6		2.0
	1.25		4.0		1.8
	1.4		4.5		1.6

MICROCOPY RESOLUTION TEST CHART  
NATIONAL BUREAU OF STANDARDS 1963-A

DEPARTMENT OF MECHANICAL ENGINEERING AND MECHANICS  
SCHOOL OF ENGINEERING  
OLD DOMINION UNIVERSITY  
NORFOLK, VIRGINIA

CONTROL OF LARGE SPACE STRUCTURES AND  
ASSOCIATED PRECISION-POINTED PAYLOADS

By

S.M. Joshi

G.L. Goglia, Principal Investigator

Annual Progress Report  
For the period February 15, 1981 to February 14, 1982

Prepared for the  
National Aeronautics and Space Administration  
Langley Research Center  
Hampton, Virginia 23665

Under  
Research Grant NAG-1-102  
Harold A. Hamer, Technical Monitor  
Flight Dynamics and Control Division

Submitted by the  
Old Dominion University Research Foundation  
P.O. Box 6369  
Norfolk, Virginia 23508-0369



May 1982

CONTROL OF LARGE SPACE STRUCTURES AND  
ASSOCIATED PRECISION-POINTED PAYLOADS

By

S.M. Joshi\*

ABSTRACT

Stability and robustness of a two-level control system for large space structures were investigated. In particular, the effects of actuator/sensor nonlinearities and dynamics on the closed-loop stability were studied and the problem of control-systems design for fine-pointing of several individually pointed payloads mounted on a large space platform was examined. A composite controller was proposed and was stable and robust.

INTRODUCTION

The basic problems in attitude control of large space structures (LSS)--in the context of control of relatively rigid conventional spacecraft--have been known for several years and have been formally brought into focus recently. Because of the pointing requirements, it is necessary to have LSS closed-loop, rigid-body bandwidth higher than a number of structural modal frequencies. A practical controller can be designed to actively control only a few of the infinite structural modes. Stability of the closed-loop system depends heavily on the inherent structural damping, particularly in the uncontrolled or residual modes (Joshi and Groom, 1979). Inherent damping ratios are difficult, if not impossible, to predict. Therefore, it is highly desirable to increase the structural damping of LSS using a secondary or damping enhancement controller. Because of the lack of accurate knowledge of the structural parameters, the ideal controller should be robust; that is, the closed-loop system should be stable regardless of parameter inaccuracies. This report considers a control system consisting of a primary and a secondary controller. The secondary controller

---

\*Research Associate Professor, Department of Mechanical Engineering and Mechanics, Old Dominion University, Norfolk, Virginia 23508.

enhances modal damping of the structural modes while the primary controller controls the rigid-body attitude and, possibly, some structural modes.

The literature on LSS damping enhancement proposes concepts such as direct-velocity feedback controller (Balas, 1979) and member dampers (Canavin, 1978) which use collocated actuators and sensors to provide velocity feedback that results in guaranteed Lyapunov stability. Such controllers are robust (i.e., the closed-loop system is stable regardless of parameter inaccuracies), assuming linear and infinite-bandwidth actuators and sensors. In this report, the effects of actuator/sensor dynamics as well as nonlinearities are discussed for systems employing velocity feedback.

Secondary control (i.e., damping enhancement) can also be accomplished using several Annular Momentum Control Devices (AMCDs). An AMCD (Anderson and Groom, 1975) consists of a rotating thin rim suspended in three or more noncontacting electromagnetic actuator stations and spun by a noncontacting spin-motor. The resulting closed-loop system is asymptotically stable and robust under certain conditions. A primary attitude control system that used torque-actuators and collocated attitude and rate sensors was then considered and was stable (and robust) with linear, instantaneous actuators and sensors. The effect of actuator/sensor dynamics on the primary controller was investigated.

One of the LSS concepts with significant potential is a large space platform that houses several individually pointed payloads. Possible payloads include communications, astronomy, earth resources, and weather payloads that would otherwise be installed in individual orbiting satellites. The greatest advantage of using large multimission space platforms is that the shortage of available orbital slots for communication and other satellites at geosynchronous altitudes could be alleviated. Another advantage of this concept is the cost savings of using smaller ground terminals and common payload support equipment (e.g., power, cryogenics, and data link to ground).

Fine-pointing accuracy requirements for payloads mounted on such platforms are expected to be stringent. Therefore, control-systems design for such systems is complex and challenging. The entire system consists of two subsystems: The base platform with an attitude that is controlled, but not

with great precision; and precision-pointed structures (PPS) that require highly accurate, individual fine-pointing. A large space platform (LSP) is basically a large flexible space structure; therefore, the stability of the closed-loop system with reduced-order controllers cannot, in general, be guaranteed because of control and observation "spillovers," even when the required closed-loop bandwidth is relatively low. The stability problem is further compounded by the interaction of the PPS-pointing control inputs and the LSP structural modes.

A linearized mathematical model was developed for the LSP/multiple-PPS system, where each PPS is mounted on two degree-of-freedom (DOF) gimbals; (i.e., an elevation and a lateral gimbal). A composite LSS/PSS control law was obtained with guaranteed stability and robustness.

#### LSS CONTROL: SECONDARY CONTROLLER STABILITY INVESTIGATION

##### Secondary-Controller-Using Velocity Feedback

The LSS considered in this paper are represented by a finite-order "modal model" given by:

$$\ddot{Ax} + \dot{Bx} + Cx = \gamma f \quad (1)$$

where  $x$  represents the modal amplitude vector for rigid-body as well as structural modes, and  $f$  represents the generalized force vector. Considering a large plate-like or platform-type structure, the rigid-body modes of interest are rotations about  $x$  and  $y$  axes, which are the two orthogonal in-plane axes. For this case,  $x = (\alpha_s^T, q^T)^T$ , where  $\alpha_s = (\phi_s, \theta_s)^T$  denotes the rigid-body attitude vector, and  $q$  is the  $n_q$ -dimensional modal amplitude vector.  $A, B, C$  are symmetric matrices with  $A > 0$  (positive definite),  $B > 0, C \geq 0$  (positive semidefinite), and  $\gamma$  is the  $(n_q + 2) \times n_f$  "mode shape" matrix which is determined by the values of the mode shapes at the actuator locations.

For analyzing the secondary controller using velocity feedback, consider only the flexible part of the model given by:

$$\ddot{q} + D\dot{q} + \Lambda q = \phi^T f \quad (2)$$

where  $D = D^T > 0$  represents the inherent damping matrix and  $\Lambda = \text{diag}(\omega_1^2, \omega_2^2, \dots, \omega_n^2)$ ,  $\omega_i$  being the natural frequency of mode  $i$  ("diag ( )" denotes a diagonal matrix). And  $f$  is assumed to consist only of applied torques. The attitude rate vector (assuming collocated actuators and sensors) due to flexible parts excluding sensor noise is given by:

$$y_r = \phi \dot{q} \quad (3)$$

Consider the feedback control input:

$$f = -K_r y_r = -K_r \phi \dot{q} \quad (4)$$

where  $K_r = K_r^T > 0$  is the  $n_f \times n_f$  rate feedback-gain matrix. Assuming infinite-bandwidth linear actuators and sensors, the closed-loop system given by equations (2) and (4) is Lyapunov-stable if  $K_r > 0$ , and is asymptotically stable if  $K_r > 0$  and  $(\Lambda, \phi^T)$  is controllable (Aubrun et al., 1979). This controller is robust (stable regardless of parameter inaccuracies and number of modes in the model). However, the stability is no longer guaranteed when the actuators and sensors have finite bandwidth and possibly nonlinear characteristics. The following sections address these problems.

#### Effect of Nonlinear Actuator/Sensor Characteristics

Assuming that the signal path containing sensors and actuators has time-invariant nonlinearities as shown in the block diagram of Figure 1, the actual control input is given by:

$$f = -\Psi_a \left\{ K_r \Psi_s(\sigma) \right\} = -\Psi_a(\sigma_a) \quad (5)$$

where

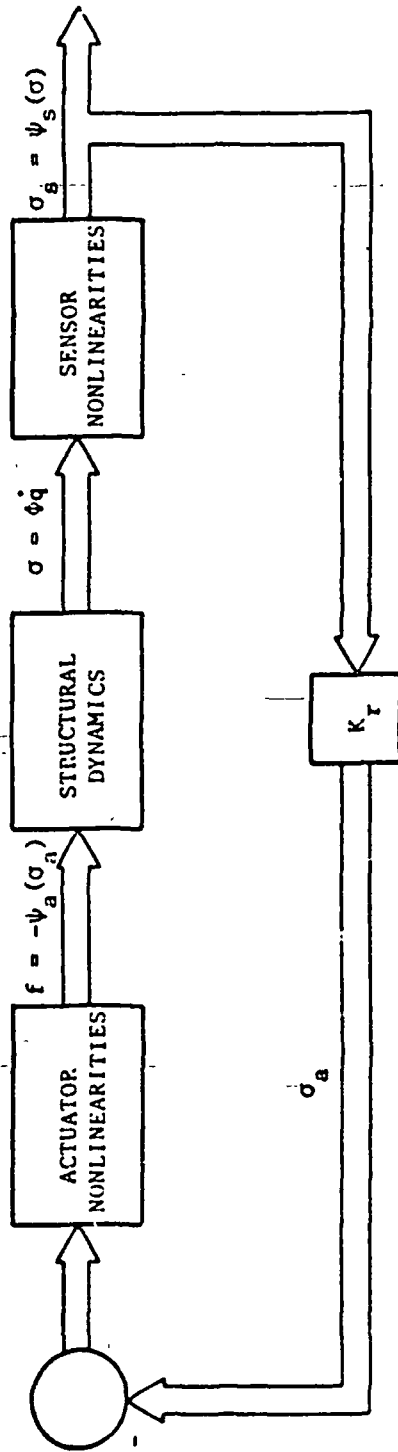


Figure 1. Velocity feedback controller.



$$\sigma = \dot{\phi}q, \sigma_a = K_r \Psi_s(\sigma) \quad (6)$$

$\Psi_a$  and  $\Psi_s$  represent the actuator and sensor nonlinearities and are  $(n_f \times 1)$  vector-valued functions of vector arguments. The  $i$ th component  $\Psi_{a_i}$  of  $\Psi_a$  is a function only of the corresponding component of  $\sigma_a$ . The same holds for  $\Psi_s$ . Also, let  $\Psi_a(0) = \Psi_s(0) = 0$ . Considering the worst case with  $D = 0$ , the closed-loop system is given by:

$$\ddot{q} + \Lambda q + \dot{\phi}^T \Psi_a(\sigma_a) = 0 \quad (7)$$

Consider first the case with linear sensors and nonlinear actuators:

**THEOREM 1.** a. In the case of linear sensors, the origin of the system of equation (7) is stable if  $K_r > 0$  and  $\sigma_a^T K_r^{-1} \Psi_a(\sigma_a) > 0$ . b. The origin is asymptotically stable in the large (ASIL) if  $K_r > 0$ ,  $\sigma_a^T K_r^{-1} \Psi_a(\sigma_a) > 0$  for  $\sigma_a \neq 0$  and  $(\Lambda, \dot{\phi}^T)$  is controllable.

Proof. Consider a Lyapunov function:

$$V = q^T \Lambda q + \dot{q}^T \dot{q} \quad (8)$$

a. It can be proved that:

$$\dot{V} = 2\sigma_a^T K_r^{-1} \Psi_a(\sigma_a) < 0 \quad (9)$$

b. In this case,  $\dot{V} < 0$  except possibly when  $\sigma_a = 0$ . It can be shown that that  $\sigma_a \neq 0$  except at the origin, since  $(\Lambda, \dot{\phi}^T)a$  is controllable. If  $K_r$  is diagonal, the nonlinearities merely have to be confined to the first and the third quadrants as shown in Figure 2 (i.e.,  $\sigma \Psi_{a_i}(\sigma) > 0$ ,  $\sigma \neq 0$ , for ASIL). The effect of nonlinearities in both sensors and actuators is considered next.

**THEOREM 2.** If  $K_r = \text{diag}(K_{r_1}, K_{r_2}, \dots, K_{r_{n_f}})$ , and  $\sigma \Psi_{a_i}(\sigma) > 0$ ,  $\sigma \Psi_{s_i}(\sigma) > 0$  for  $\sigma \neq 0$ , then the origin of the closed-loop system of equation (7) is stable if  $K_{r_i} > 0$ , and is ASIL if, in addition,  $(\Lambda, \dot{\phi}^T)$  is controllable.

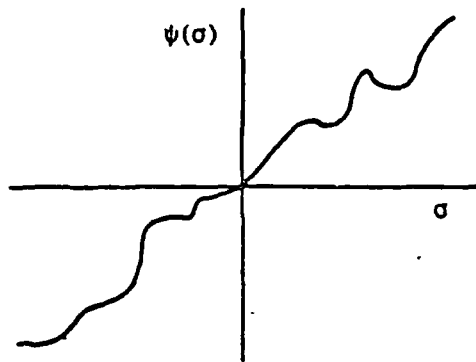


Figure 2. Sector-type nonlinearity.

Proof. Proceeding as in the proof of THEOREM 1, it can be shown that:

$$\dot{V} = - \sum_{i=1}^{n_f} \sigma_{a_i} \Psi_{a_i}(\sigma_{a_i}) \left( \frac{\sigma_i}{\Psi_{s_i}(\sigma_i)} \right) \frac{1}{K_{r_i}}$$

The rest of the proof is similar to that of THEOREM 1.

#### Effect of Actuator and Sensor Dynamics

Assuming the sensors and actuators are linear but have finite bandwidth, the closed-loop equations can be written as:

$$\ddot{q} + D\dot{q} + \Lambda q = \Phi^T f \quad (10a)$$

$$f = C_a x_a \quad (10b)$$

$$\dot{x}_a = A_a x_a + B_a U_a \quad (10c)$$

$$U_a = -K_r \dot{\phi} q \quad (10d)$$

where  $x_a$ ,  $U_a$  are  $n_a \times 1$  and  $n_f \times 1$ , actuator/sensor (combined) state and input vectors, and  $A_a$ ,  $B_a$ ,  $C_a$  are the system input and output matrices, with  $A_a$  being strictly Hurwitz. The steady-state gain is unity; that is:

$$C_a A_a^{-1} B_a = -I \quad (11)$$

With instantaneous actuators/sensors, the system is guaranteed to be asymptotically stable (AS) if  $K_r > 0$  and  $(\Lambda, \Phi^T)$  is controllable. (For linear systems, AS and ASIL are equivalent.) However, it may be unstable when the actuators/sensors have dynamic characteristics as in equation (10). Suppose the actuator/sensor system equation can be represented by:

$$\dot{\mu} x_a = A_a x_a + B_a U_a \quad (12)$$

where  $\mu$  is a small positive scalar. If the closed-loop system with perfect actuators/sensors is AS, it can be shown that the trajectory with finite bandwidth is  $O(\mu)$  close to the trajectory with perfect actuators/sensors (Chow and Kokotovic, 1976). This result implies that if the actuator/sensor bandwidth is sufficiently high, the closed-loop system would be AS; however, it does not provide a method for determining a quantitative measure of  $\mu$  that will guarantee stability.

The multivariable stability problem of equation (10) does not appear to lend itself to useful generic solutions. It is therefore instructive to investigate at this point the single-input, single-output (SISO) system. In this case,  $n_f = 1$  in equation (10), and  $K_r$  is a scalar. Let  $G_a(s)$  denote the transfer function that represents the combined actuator/sensor dynamics. In order to consider the worst case, let  $D = 0$ . It is assumed for simplicity that LSS has no repeated modal frequencies and no pole-zero cancellations (i.e., controllability). The following results offer some insight into actuator/sensor bandwidth requirements.

**THEOREM 3.** The system of equation (10) is AS for sufficiently small  $K_r > 0$  iff (if and only if) the phase  $\phi_a(\omega)$  of  $G_a(j\omega)$  is such that  $-90^\circ < \phi_a(\omega) < 90^\circ$  for  $\omega = \omega_i, i = 1, 2, \dots, n_q$ .

Proof. The proof can be established by examining the root-locus angles of departure at the LSS open-loop poles, which are at  $\pm j\omega_i, i = 1, 2, \dots, n_q$ .

It is clear that for unrealistic actuators/sensors this condition cannot be satisfied for an infinite number of undamped structural modes. In reality, however, some inherent damping is always present and it is generally higher for higher-frequency modes.

If  $G_a(s)$  has no finite zeros and  $n_a$  no real poles at  $s = -\sigma_a$ , the closed-loop system is AS for sufficiently small  $K_r > 0$  iff, denoting the largest  $\omega_i$  by  $\omega_M$ :

$$\sigma_a > \omega_M / \tan(\pi/2n_a) \quad (13)$$

Table 1 shows the minimum  $\sigma_a / \omega_M$  required for stability for different  $n_a$ . The above results use only the information about the LSS modal frequencies. However, considerable additional investigation is necessary in this area to obtain more useful results, especially for the multivariable

Table 1. Actuator/sensor bandwidth requirements for velocity feedback.

Actuator/Sensor Order $n_a$	1	2	3	4	5	6	7	8
$\sigma_a / \omega_M >$ (Min. Req'd.)	0	1	1.73	2.48	3.09	3.76	4.37	5.07

case. Perhaps newly emerging techniques such as multivariable frequency-domain methods (Postlethwaite and MacFarlane, 1979) may be useful in these investigations.

### Secondary Controller Using AMCDs

The use of an AMCD for damping enhancement was proposed by Joshi and Groom (1980a, 1980b). The use of several AMCDs for secondary control was investigated by Joshi (1980). The AMCDs considered are assumed to have relatively small rim diameters (about 2 m) and are therefore rigid. Electromagnetic force actuators and rim-proximity sensors used for the AMCDs exhibit a high degree of linearity in the operating range and have bandwidths of several hundred Hz. Therefore, the AMCD actuators and sensors can be assumed to be linear and instantaneous.

The control system configuration consists of several AMCDs distributed on the LSS. As shown in Figure 3, each AMCD consists of a rotating thin rim suspended in three or more noncontacting electromagnetic force actuators which can exert the commanded forces in the z-direction. A z-axis rim proximity sensor, which measures the relative displacement between the rim and the LSS, is installed at the location of each actuator.

The complete linearized equations of motion were developed by Joshi (1981a). Consider the control law given by:

$$f_A = K_P \delta + K_R \dot{\delta} \quad (14)$$

where  $f_A$  and  $\delta$  represent  $l \times 1$  vectors of actuator forces and proximity sensor outputs for all AMCDs. Where  $l$  is the total number of AMCD actuators,  $K_P$  and  $K_R$  denote  $l \times l$  symmetric gain matrices. The closed-loop system state vector consists of  $z$  and  $\dot{z}$ , where

$$z = (\alpha_s^T, \alpha_{a_1}^T - \alpha_s^T, \dots, \alpha_{a_v}^T - \alpha_s^T, \epsilon_1, \dots, \epsilon_v)^T \quad (15)$$

where  $\alpha_{a_i} = (\phi_{a_i}, \theta_{a_i})^T$  represents the attitude vector of the  $i$ th AMCD rim ( $v$  = number of AMCDs) and  $\epsilon_i$  represents the z-axis displacement of the  $i$ th AMCD rim center relative to the corresponding point fixed to LSS. It

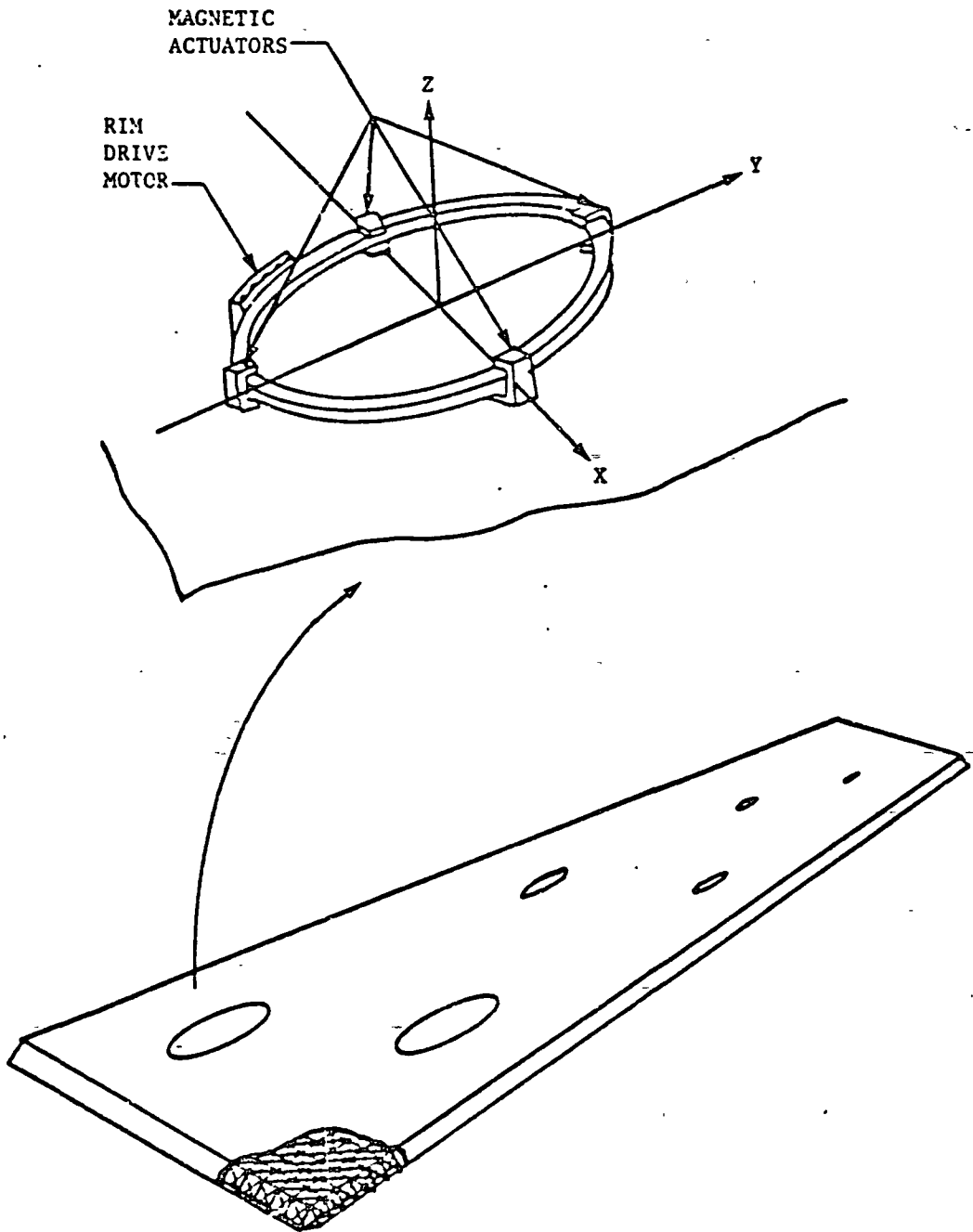


Figure 3. AMCD/LSS configuration.

was proved (Joshi, 1981a) that the closed-loop system is stable if  $K_p > 0$ ,  $K_r > 0$ , and is AS if (1)  $K_p > 0$ ,  $K_r > 0$ ; (2) the LSS structural model is stabilized; (3) the total z-axis angular momentum of the AMCDs is nonzero; and (4) LSS has no undamped structural modes at twice the AMCD spin frequencies. The secondary controller using AMCDs is stable and robust. The amount of damping enhancement in different modes will depend on the value of the mode shapes at the actuator locations. If several AMCDs are distributed on the LSS, structural damping of a number of modes can be enhanced. The hardware required for this type of secondary controller is within the reach of present-day technology (Groom and Terray, 1978).

#### LSS CONTROL: PRIMARY ATTITUDE CONTROL SYSTEM

The secondary system increases modal damping and thus controls the shape of the LSS. It also aids in primary controller design by reducing the effects of "spillover" (Balas, 1978). A primary attitude control system using instantaneous torque actuators and attitude and rate sensors is considered first.

##### Primary Controller Using Collocated Actuators/Sensors

Assuming that primary attitude control is accomplished using  $m (>1)$ , two-axis torque actuators distributed on the LSS, the LSS equations of motion (without secondary controller) are given by:

$$\ddot{Ax} + B\dot{x} + Cx = \Gamma T \quad (16)$$

where  $T$  is the  $m \times 1$  torque vector. For collocated attitude sensors, the total attitude vector (including the contributions of rigid-body and flexible modes) is given by:

$$\alpha_t = \Gamma^T x \quad (17)$$

Consider the control law:

$$T = -(G_p \alpha_t + G_r \dot{\alpha}_t) \quad (18)$$



where  $G_p$  and  $G_r$  are symmetric matrices. It can be proved that the closed-loop system--equations (16) and (18)--is AS if  $G_p > 0$ ,  $G_r > 0$ , and  $(C, \Gamma)$  is controllable. It is of interest to note that the control law of equation (18) minimizes a linear quadratic (LQ) performance index (with infinite terminal time), which has a state-control, cross-penalty term in addition to quadratic penalties on the state and the control vectors. (The proof can be obtained in a manner similar to Joshi, 1981a.) The controller is AS regardless of parameter inaccuracies. However, the stability is not guaranteed if the actuators/sensors have finite bandwidth. Consider the SISO case of a single torque actuator and collocated attitude and rate sensors. Assuming that the LSS does not have repeated modal frequencies (except at the origin), that  $(\Lambda, \Phi^T)$  is controllable, and that  $G_p = k g_p$ ,  $G_r = k g_r$  ( $g_p, g_r, k$  are positive scalars), the following results can be obtained (provided that  $\phi_a(0) = 0$ ).

#### DESIGN OF STABLE CONTROLLERS FOR LSS

**THEOREM 4.** For the system given by equations (16) and (18), the closed-loop poles corresponding to the structural modes have negative real parts for arbitrarily small  $k > 0$  iff

$$-\phi_{z_i} < \phi_a(\omega_i) < 180^\circ - \phi_{z_i} \quad (19)$$

for  $i = 1, 2, \dots, n_q$ , where  $\phi_{z_i} = \arctan(\omega_i g_r / g_p)$ .

**Proof.** The proof can be obtained by examining the root-locus angles of departure at  $\pm j\omega_i$ . The actuator/sensor dynamics do not affect the angles of departure for the poles at the origin.

If  $G_a(s)$  has no zeros and  $n_a$  has no poles at  $s = -\sigma_a$ , the system is AS if  $\arctan(\omega_i / \sigma_a) > -\phi_{z_i} / n_a$  for  $i = 1, 2, \dots, n_q$ . Further investigation is needed in order to obtain useful results in the area. Also, the effect of nonlinearities in primary actuators/sensors needs investigation.

### Primary Controller Using Noncollocated Actuators/Sensors

The stability of the closed-loop system is no longer guaranteed for this case, even with perfect actuators and sensors. This is because of control and observation "spillovers" (Balas, 1978). For the noncollocated case, the primary controller design can be accomplished using methods based on linear-quadratic Gaussian (LQG) control theory. Joshi and Groom (1979) presented and discussed several methods based on LQG theory. Of these methods, the modified truncation or model-error sensitivity suppression (MESS) method, which was first proposed by Sesak, Likins, and Cordadetti (1979) was found to be the most promising. In this method, the effect of control input on selected residual modes is included in the performance function in a quasi-static sense. The resulting reduced-order linear quadratic optimal regulator problem has a term that modifies the control-weighting matrix in the performance index. A modified state estimator can also be designed in a similar manner. A more detailed discussion can be found in (Sesak, Likins, and Cordadetti, 1979). Numerical results for a large, thin, completely free, flat plate (for the collocated and noncollocated cases) are given by Joshi (1981a).

### Primary Attitude Control Using AMCDs

The AMCDs used for the secondary controller can be used simultaneously for actuation of the primary attitude controller. Primary attitude control is accomplished by torquing against the AMCD angular momenta. In this dual control mode, however, the relative rotation angles between LSS and AMCDs (i.e.,  $\alpha_{a_i} - \alpha_s$ ,  $i = 1, 2, \dots, \nu$ ) cannot be controlled simultaneously with LSS rigid-body attitude  $\alpha_s$ . Joshi (1981) presented a method of structuring the position feedback gain matrix  $K_p$  in such a manner that the closed-loop secondary system with the state vector consisting of  $e_i, \dot{e}_i, \dot{\alpha}_{a_i} - \dot{\alpha}_s$  ( $i = 1, 2, \dots, \nu$ ) is guaranteed Lyapunov-stable. Additional force commands can be superimposed on the electromagnetic actuators in order to produce the desired primary attitude control torques for controlling  $\alpha_s$ . If an attitude and a rate sensor is placed on the LSS at the nominal position of the center of each AMCD, this configuration would approximate collocated point-torque actuators and attitude/rate sensors, and should have the associated stability and robustness properties. In this configuration, the

AMCDs must have sufficiently large momenta in order to exert the magnitude of torques required to achieve the desired rigid-body bandwidth without exceeding the electromagnetic actuator gap limits. Separate AMCDs may also be used for primary control actuation. For orbital application it will be necessary to gimbal the AMCDs for primary controller actuation.

#### LSP/MPPS MATHEMATICAL MODEL

The first step toward the solution of the problem of simultaneous control of LSP attitude and PPS fine-pointing was to derive a linear mathematical model for the system consisting of LSP and precision-pointed payloads. Each payload (PPS) is rigidly mounted on a lateral gimbal which is attached to an elevation gimbal. Each elevation gimbal is rigidly attached to the LSP. Each elevation gimbal can rotate about the LSP x-axis, and each lateral gimbal can rotate about the y-axis of the corresponding elevation gimbal. Each gimbal also has a torquer. (The roll freedom of payload is not considered in this analysis.) The LSP attitude is assumed to be controlled by  $n$  torque actuators distributed on the LSP. The mathematical model derived below assumes that each PPS is rigid, and is treated as a point mass for the purpose of LSP structural model computation. The LSP/MPPS model derived via Lagrangian formulation has the following form:

$$\ddot{\mathbf{x}} + \mathbf{B}\dot{\mathbf{x}} + \mathbf{C}\mathbf{x} = \mathbf{\Gamma}\mathbf{f} \quad (20)$$

where

$$\mathbf{x} = (\phi_s, \theta_s, \psi_s, \phi_1, \phi_2, \dots, \phi_p, \theta_1, \theta_2, \dots, \theta_p, \mathbf{q}^T)^T \quad (21)$$

where  $\phi_s, \theta_s, \psi_s$  (which will be denoted by the vector  $\alpha_s$ ) are the LSP rigid-body roll, pitch, and yaw angles (about x, y, z axes). The relative angles between each elevation gimbal and LSP are  $\phi_1, \dots, \phi_p$  (to be denoted by  $\phi$ ); and  $\theta_1, \dots, \theta_p$  (to be denoted by  $\theta$ ) are the lateral gimbal angles. The  $n_q \times 1$  LSP modal amplitude vector is  $\mathbf{q}$ .

$$A = \left[ \begin{array}{ccc|c} (A_{11})_{3 \times 3} & A_{12} & A_{13} & 0 \\ A_{21} & (A_{22})_{p \times p} & A_{23} & 0 \\ A_{31} & A_{32} & (A_{33})_{p \times p} & 0 \\ \hline 0 & 0 & 0 & I_{n_q \times n_q} \end{array} \right] \quad (22)$$

The  $A_{ij}$  matrices are appropriately dimensional submatrices

$$B = \left[ \begin{array}{c|c} 0 & 0 \\ \hline 0 & D \end{array} \right] \quad (23)$$

$$D = DT > 0$$

which is the  $n_q \times n_q$  large space structure (LSS) inherent damping matrix.

$$C = \left[ \begin{array}{c|c} 0 & 0 \\ \hline 0 & \Lambda \end{array} \right] \quad (24)$$

$$\Lambda = \text{diag}(\omega_1^2, \omega_2^2, \dots, \omega_{n_q}^2) \quad (25)$$

where  $\omega_i$  denotes the  $i$ th modal frequency of the LSP. Assuming that the LSP is controlled by  $m$  two-axis ( $x$  and  $y$ ) torque actuators,

$$f = (T_1^T, T_2^T, \dots, T_m^T, T_{e1}, T_{e2}, \dots, T_{ep}, T_{l1}, T_{l2}, \dots, T_{lp})^T \quad (26)$$

where  $T_i = (T_{xi}, T_{yi})^T$  represents the  $i$ th LSP control torque vector and  $T_{ei}, T_{li}$  represent the  $i$ th elevation and lateral gimbal torquer torques.

$$\Gamma = \left[ \begin{array}{ccc|c} I_{2 \times 2}, \dots, I_{2 \times 2} & -e_1, -e_1, \dots, -e_1 & -T_{11}^T e_2, \dots, -T_{1p}^T e_2 \\ 0_{1 \times 2}, \dots, 0_{1 \times 2} & & & \\ \hline 0 & I_{p \times p} & 0 & \\ \hline 0 & 0 & I_{p \times p} & \\ \hline \psi^T & \tau_x & \tau_y & T_d \end{array} \right] \quad (27)$$

where  $T_{1_i} = T_1(\phi_{oi})$  is the transformation matrix for rotation  $\phi_{oi}$  about x-axis, where  $\phi_{oi}$  = nominal angle of the ith gimbal relative to the LSP. The  $3 \times 1$  unit vector in k-direction is denoted by  $e_k$ . The  $n_q \times 2m$  mode shape matrix for LSP torque actuator locations is denoted by  $\psi^T$ . The  $n_q \times p$  matrices of mode shapes (in x and y directions) at the elevation gimbal locations are  $\psi_x^T$  and  $\psi_y^T$ .

$$T_d = \text{diag} [T_{11}(2,2), T_{12}(2,2), \dots, T_{1p}(2,2)] \quad (28)$$

### Sensor Outputs

It is assumed that  $m$  attitude and rate sensors are collocated with the LSP control torque actuators. The LSP attitude sensor output for the  $i$ th sensor is given by:

$$y_{si} = \frac{\dot{\phi}_s}{\theta_s} + \psi_i q \quad (29)$$

where  $\psi_i$  denotes the  $2 \times n_q$  submatrix of  $\psi$  corresponding to  $i$ th sensor location. Assuming that each payload has its own attitude and rate sensor, it can be shown that the (2-vector) output of the  $i$ th payload attitude sensor is given by:

$$y_{pi} = \begin{bmatrix} \cos \theta_{oi} & 0 \\ 0 & 1 \end{bmatrix} \begin{bmatrix} \phi_i \\ \theta_i \end{bmatrix} + \begin{bmatrix} \cos \theta_{oi} & 0 & -\sin \theta_{oi} \\ 0 & 1 & 0 \end{bmatrix} \begin{bmatrix} \dot{\phi}_s + \psi_{xi} q \\ \dot{\theta}_s + \psi_{yi} q \\ \dot{\psi}_s \end{bmatrix} \quad (30)$$

where  $\theta_{oi}$  is the nominal gimbal angle for the  $i$ th lateral gimbal. Gimbal angles  $\phi_i$  and  $\theta_i$  are also measured. They denote the incremental gimbal angles about  $(\phi_{oi}$  and  $\theta_{oi})$  in this linearized analysis.

## CONTROL SYSTEMS SYNTHESIS FOR LSP/MPPS

### Control Law I: Decentralized Control

In this method, the LSP attitude and the PPS attitude are controlled independently. The LSP attitude and vibration control can be accomplished using a two-level controller with collocated actuators and sensors. Each PPS control system is designed independently and incorporates feedback only of the PPS attitude and rate signals in order to generate the gimbal torquer torque commands. An examination of the A matrix in equation (22) indicates that strong couplings exist not only between the LSP and all the PPSs but also between the PPSs themselves. Additional coupling, including that due to LSP flexibility, would also be introduced by the feedback control law. Since the masses of individual PPSs can be large (i.e., of the same order as the LSP mass), overall instability may occur for this type of decentralized control law.

### Control Law II: Robust Composite Control

The sensor outputs described above can be combined in the following manner:

$$z_1 = [y_{s_1}^T, y_{s_2}^T, \dots, y_{s_m}^T]^T \quad (31)$$

where  $y_{s_i}$  is the LSP attitude measurement equation (29) at the  $i$ th LSP sensor location.

$$z_2 = [z_{21}^T, z_{22}^T, \dots, z_{2p}^T]^T \quad (32)$$

where

$$z_{2i} = 2\phi_i - \sec \theta_{oi} (\phi_{pi} + \sin \theta_{oi} \psi_s) \quad (33)$$

On expansion it can be seen that:

$$z_{2i} = \phi_i - (\phi_s + \psi_{xi} q) \quad (34)$$

$$z_j = [z_{j1}^T, z_{j2}^T, \dots, z_{jp}^T] \quad (35)$$

where

$$z_{ji} = z_{\theta_i} - \theta_{pi} \quad (36)$$

It should be noted that LSP yaw angle measurement ( $\psi_B$ ) is required to generate  $z_2$ . Denoting

$$z = (z_1^T, z_2^T, z_3^T)^T \quad (37)$$

it can be shown that:

$$\dot{z} = \Gamma^T x \quad (38)$$

Consider the control law:

$$\dot{f} = -K_p z - K_r \dot{z} \quad (39)$$

where  $K_p$  and  $K_r$  are symmetric matrices.

**THEOREM 5.** If  $K_p > 0$  (positive definite) and  $K_r > 0$  (positive semidefinite), then the closed-loop system given by equations (20) and (39) (but excluding the LSP yaw angle  $\psi_B$ ) is stable in the sense of Lyapunov.

Proof. The proof is similar to that of THEOREM 1 in (Joshi, 1981b).

The controller is robust because it assures stability regardless of parameter inaccuracies and number of structural modes in the LSP model.

#### NUMERICAL RESULTS--LSP/PPS CONTROL

In order to investigate the two controllers discussed, a finite element model of a 100-ft. x 100-ft. x 0.1-in. completely free, aluminum plate was used to represent a large space platform. Two payloads, with masses equal to that of the LSP, were assumed to be located at different points on the

LSP. The payloads were assumed to be nominally pointing at targets  $45^\circ$  and  $-45^\circ$  respectively about the inertial x-axis, and  $0^\circ$  about the y-axis of the elevation gimbals for this stimulation. The LSP was assumed to be controlled by three torque actuators (each two-axis) collocated with attitude and rate sensors. For the purpose of this analysis, the LSP structural model was not modified by adding point masses at PPS locations, the purpose being only to demonstrate the methods rather than to obtain accurate numerical results. The objective was to get LSP rigid-body, closed-loop bandwidth of about 0.05 rad/sec with damping ratio of about 0.707, and flexible mode damping ratio of at least 10% (zero open-loop damping assumed). The PPS closed-loop bandwidth was required to be 1 rad/sec with 0.707 damping. The closed-loop eigenvalues for the two controllers were obtained for various attitude and rate gains (assumed to be diagonal matrices) for LSP and PPS. When the PPS gains were raised (for obtaining the required 1 rad/sec closed-loop bandwidth for the PPS loop), a structural mode was driven unstable in the decentralized controller for PPS bandwidth greater than 0.18 rad/sec. The composite controller was next used. In this case, PPS bandwidth of 1 rad/sec was obtained without significantly affecting any of the structural modes. Work is currently in progress in order to fully evaluate the performance of the controllers.

#### CONCLUDING REMARKS

The effects of sensor and actuator nonlinearities and dynamics on the stability of the two-level controller were investigated. The secondary controller was shown to be robust in the presence of sector-type, memoryless sensor/actuator nonlinearities. Further investigation is needed for (1) the effects of nonlinearities on the primary controller, and (2) the effects of sensor/actuator dynamics for the multi-input, multi-output case (for both the primary and the secondary controllers). Two types of controllers--a decentralized controller and a robust composite controller--were considered for the control of LSP/PPS system. The robust composite controller offers significant promise. The performance of the controllers is currently under investigation.



## REFERENCES

- Anderson, W.W.; and Groom, N.J.: The Annular Momentum Control Device (AMCD) and Potential Applications. NASA TND-7866, March 1975.
- Aubrun, J.R.; Lyons, M.; Marguiles, G.; Arbel, A.; and Gupta, M.: Stability Augmentation for Flexible Space Structures. Proceedings, 18th IEEE Conference on Decision and Control, Ft. Lauderdale, Florida, 1979.
- Balas, M.J.: Direct Velocity Feedback Control of Large Space Structures. AIAA J. Guidance and Control, vol. 2, no. 3, 1979, pp. 252-253.
- Balas, M.J.: Feedback Control of Flexible Systems. IEEE Trans. Autom. Control, vol. 23, no. 4, 1978, pp. 673-679.
- Canavin, J.R.: Control Technology for Large Space Structures. Proceedings, AIAA Conference on Large Space Platforms, Los Angeles, California, 1978.
- Chow, J.H.; and Kokotovic, P.V.: A Decomposition of Near-Optimum Regulators for Systems with Slow and Fast Modes. IEEE Trans. Autom. Control, vol. 21, no. 5, 1976, pp. 701-705.
- Groom, N.J.; and Terray, D.E.: Evaluation of a Laboratory Test Model Annular Momentum Control Device. NASA TR-1142, 1978.
- Joshi, S.M.: A Controller Design Approach for Large Space Structures. NASA CR-165717, 1981a.
- Joshi, S.M.: Damping Enhancement and Attitude Control of Large Space Structures. Proc. 19th IEEE Conference on Decision and Control, Albuquerque, New Mexico, 1980.
- Joshi, S.M.: Design of Stable Feedback Controllers for LSS. Third VPISU/AIAA Symposium on Dynamics and Control of Large Flexible Spacecraft, Blacksburg, Virginia, 1981b.
- Joshi, S.M.; and Groom, N.J.: Controller Design Approaches for Large Space Structures Using LQG Control Theory. Proc. Second VPISU/AIAA Symposium on Dynamics and Control of Large Flexible Spacecraft, Blacksburg, Virginia, 1979, pp. 35-50.
- Joshi, S.M.; and Groom, N.J.: Modal Damping Enhancement in Large Space Structures Using AMCDs. AIAA J. Guidance Control, vol. 3, no. 5, 1980a, pp. 477-479.
- Joshi, S.M.; and Groom, N.J.: A Two-Level Controller Design Approach for Large Space Structures. Proc. 1980 Joint Automatic Control Conference, San Francisco, California, 1980b.
- Postlethwaite, I.; and MacFarlane, A.G.J.: A Complex Variable Approach to the Analysis of Linear Multivariable Feedback Systems. Springer (Berlin), 1979.

Sesak, J.R.; Likins, P.W.; and Cordadetti, T.: Flexible Spacecraft Control by Model Error Sensitivity Suppression (MESS). J. Astronautical Sciences, vol. 27, no. 2, 1979, pp. 131-156.

END  
DATE  
FILMED

JUL 28 1982

1 OF 1

N82-24280 UNCLAS

